Asian dust particles converted into aqueous droplets under remote marine atmospheric conditions

PHYSICAL SCIENCES - Environmental Sciences

Asian dust particles converted into aqueous droplets under remote marine atmospheric conditions

Yutaka Tobo[a, 1], Daizhou Zhang[b], Atsushi Matsuki[a], and Yasunobu Iwasaka[a, 1]

[a]Frontier Science Organization, Kanazawa University, Kanazawa, Ishikawa 920-1192, Japan; and [b]Faculty of Environmental and Symbiotic Sciences, Prefectural University of Kumamoto, Kumamoto 862-8502, Japan

[1]To whom correspondence should be addressed.

Frontier Science Organization, Kanazawa University, Kanazawa, Ishikawa 920-1192, Japan

Tel. & Fax: +81-76-234-4645

E-mail: ytobo@staff.kanazawa-u.ac.jp or kosa@staff.kanazawa-u.ac.jp

The chemical history of dust particles in the atmosphere is crucial for assessing their impact on both the Earth's climate and ecosystem. So far, a number of studies have shown that, in the vicinity of strong anthropogenic emission sources, Ca-rich dust particles can be converted into aqueous droplets mainly by the reaction with gaseous HNO_3 to form $Ca(NO_3)_2$. Here we show that other similar processes have the potential to be activated under typical remote marine atmospheric conditions. Based on field measurements at several sites in East Asia and thermodynamic predictions, we examined the possibility for the formation of two highly soluble calcium salts, $Ca(NO_3)_2$ and $CaCl_2$, which can deliquesce at low relative humidity. According to the results, the conversion of insoluble $CaCO_3$ to $Ca(NO_3)_2$ tends to be dominated over urban and industrialized areas of the Asian continent, where the concentrations of HNO_3 exceed those of HCl ($[HNO_3/HCl] > \sim 1$). In this regime, $CaCl_2$ is hardly detected from dust particles. However, the generation of $CaCl_2$ becomes detectable around the Japan Islands, where the concentrations of HCl are much higher than those of HNO_3 ($[HNO_3/HCl] < \sim 0.3$). We suggest that elevated concentrations of HCl in the remote marine boundary layer are sufficient to modify Ca-rich particles in dust storms and can play a more important role in forming a deliquescent layer on the particle surfaces as they are transported toward remote ocean regions.

¥body

Desert dust storms contribute episodically to the global aerosol load (1, 2) and influence the radiative balance, ice nuclei and cloud condensation nuclei prevalence in the atmosphere (3, 4), and also atmospheric deposition of nutrients and toxicants (5, 6). Dust particles at their original source regions consist principally of insoluble particles and therefore serve as one of the most effective ice nuclei that initiate ice-crystal formation under cirrus conditions (7, 8). However, if dust particles are coated with soluble materials (i.e., antifreeze agents), then this process is expected to reduce their original ice-nucleating ability (9, 10), as well as enhance their liquid cloud-nucleating ability (11-15) and modify their light scattering and absorption ability (14-16). It has also been suggested that dust particles that contain certain soluble materials (e.g., iron, nitrate and phosphate) have the potential to stimulate phytoplankton growth in the open ocean (5), while some of them (e.g., copper) may cause a toxic effect (6).

There are two major pathways for the formation of soluble materials on the surfaces of dust particles: coagulation of dust and ambient soluble particles, and heterogeneous reactions of dust particles with ambient reactive gases. Thermodynamic studies suggest that alkaline $CaCO_3$ can react with gaseous HNO_3 and HCl to form $Ca(NO_3)_2$ and $CaCl_2$ (17). Both $Ca(NO_3)_2$ and $CaCl_2$ are highly soluble materials and much more hygroscopic than other insoluble or slightly soluble calcium salts such as $CaCO_3$, $CaSO_4$ and CaC_2O_4 (18). In the bulk, the anhydrous $Ca(NO_3)_2$ and $CaCl_2$ are transformed into the crystalline hydrates at relative humidity (RH) higher than 9%RH and 0.6%RH, and then deliquesce above 50%RH and 28%RH, respectively (17). In addition, it becomes clear that micrometer-sized $Ca(NO_3)_2$ particles can deliquesce above ~10%RH without the formation of the hydrates (19, 20). Thus, the deliquescent relative humidities of $Ca(NO_3)_2$ and $CaCl_2$ are much lower than those of well-known soluble materials such as NaCl (~75%RH) and $(NH_4)_2SO_4$ (~80%RH), and both $Ca(NO_3)_2$ and $CaCl_2$ are likely in the form of aqueous liquid under most conditions of the atmospheric boundary layer.

There are many unanswered questions concerning heterogeneous reactions to form aqueous droplets of $Ca(NO_3)_2$ and/or $CaCl_2$ from Ca-rich dust particles under atmospheric conditions.

3

Ca-rich dust particles that have a droplet-like (or spherical) shape have been detected at several sites of the northern hemisphere (21-26). Much of the focus on the formation of such particles so far has centered on the reaction of $CaCO_3$-containing dust particles with HNO_3 to form $Ca(NO_3)_2$ occurring in the vicinity of large anthropogenic emission sources (21-25). On the other hand, field evidence for the contribution of $CaCl_2$ has been lacking (24, 26). Furthermore, it remains controversial whether the reactions affecting the formation of $Ca(NO_3)_2$ and $CaCl_2$ can actually proceed under atmospheric conditions, largely owing to a lacking of information on the amount of atmospheric acidic gases. In this report, we examine whether these two deliquescent calcium salts could be formed through heterogeneous pathways under atmospheric conditions at several sites in East Asia. Our results raise the possibility that $CaCl_2$ could be generated from Ca-rich dust particles by heterogeneous reactions under remote marine atmospheric conditions in the absence of strong anthropogenic emission sources.

Results

Morphology and Chemical Modification of Dust Particles. Asian dust particles mainly originate from dust storms associated with cold air outbreaks in inland arid or semi-arid areas (27). It is well known that some of them contain carbonates, which are most likely $CaCO_3$ (19, 20). According to recent chemical transport modeling studies (28), the enhanced formation of $Ca(NO_3)_2$ from solid $CaCO_3$-containing dust particles is likely to take place in the atmosphere over the eastern (urban and industrialized) areas of the Asian continent (see red contour lines in Fig. 1A). In fact, Ca-rich dust particles that have a droplet-like shape and contain rich nitrate (most likely, $Ca(NO_3)_2$) have been detected previously in the polluted boundary layer of these areas, such as Beijing, China (22-24), and Chuncheon, Korea (25). The location of these sites is shown in Fig. 1A. Although these field studies conclude that the results are attributed to the formation of $Ca(NO_3)_2$, only Li and Shao (24) carefully evaluate the content of chloride in dust particles collected at Beijing. For this reason, whether such dust particles contain chloride (i.e., $CaCl_2$) or not remains a question.

Using scanning electron microscopy (SEM) with energy dispersive X-ray (EDX) analysis,

we examined the relative elemental ratios of individual dust particles from the samples collected at Beijing (the original data are taken from Matsuki et al. (22)) on April 29, 2002 (~600 m above mean sea level), and March 29, 2003 (~760 m above mean sea level). The results are plotted in a Ca:Cl:(Al + Si + Fe) ternary diagram (Fig. 1B). In these cases, Ca-free (mostly, Si- and Al-rich) particles had an irregular shape, while most of Ca-rich particles had a droplet-like shape. It is evident that these particles contained almost no chloride, corresponding to the results reported previously by Li and Shao (24). Similarly, literature data at Chuncheon (25) included Ca-rich particles that contained rich nitrate but little or no chloride. An example of the EDX analysis of the particles collected at Chuncheon is also plotted in Fig 1B. Overall, these results demonstrate that, in the eastern areas of the Asian continent, the common example of soluble materials detected in Ca-rich dust particles is certainly not $CaCl_2$ but rather $Ca(NO_3)_2$.

On the other hand, we recently reported on the existence of Ca-rich dust particles, which were very similar to the ones coated with nitrate in appearance but contained rich chloride, in the atmospheric boundary layer of Kanazawa during Asian dust storm events (26). The location of this site is shown in Fig. 1A. The results from the dust samples collected on April 21 and 24, 2007 (~150 m above mean sea level) are presented in Fig. 1C (the original data are taken from Tobo et al. (26)). The SEM images were similar to those of Beijing (Fig. 1B and refs. 22-24) and Chuncheon (25); however, the EDX analysis showed a strong correlation between Ca and Cl contents (Cl/Ca ≈ 0.315). We postulated that this correlation was attributed to partial formation of $CaCl_2$ in dust particles (26). Since Ca-rich particles presented here contained less Na and Mg (see Materials and Methods), the possibility of coagulation of dust and sea salt (i.e., NaCl or $MgCl_2$) particles should be ruled out. Also, considering the preferential detection of chloride in Ca-containing dust particles (Fig. 1C), it is highly unlikely that other non-sea salt particles (e.g., NH_4Cl) were mixed with dust particles and had a significant impact on the present results.

The SEM images of dust particles that contain rich Ca, Cl, Si and Al are illustrated in Fig. 2A (this sample was collected at Kanazawa during an Asian dust storm period on May 21, 2010). The SEM image taken at lower electron voltage (5 kV) showed that the entire picture of the particles looked like nearly droplet-like shape. Meanwhile, the SEM image taken at higher

5

electron voltage (20 kV) indicated the existence of electronically opaque core that had an irregular shape in the particles. Si and Al were detected only in the core part (most likely, aluminosilicates), but Ca and Cl were detected anywhere in the particle surfaces, suggesting that the particles were coated with soluble materials containing $CaCl_2$ (see Fig. 2 *B* and *C*).

Atmospheric Gaseous HNO_3 and HCl. The results presented raise the question of whether the mechanisms responsible for the formation of Ca-rich dust particles that have a droplet-like shape could differ from area to area in East Asia. In this section, we examine the amount of highly reactive acidic gases (i.e., HNO_3 and HCl) that have the potential to induce the formation reactions of $Ca(NO_3)_2$ and $CaCl_2$.

In Fig. 1*D*, we show gaseous HNO_3 and HCl concentrations measured at several sites in East Asia from March to May, corresponding to the period when Asian dust storm events are most frequently observed. The location of the monitoring sites is shown in Fig. 1*A*. Given that there were no severe volcano eruptions in spring 2007, we believe that HNO_3 and HCl concentrations presented here are a representative example of the background values in East Asia. We divided the data into three groups: Kanghwa and Imsil, which are surrounded by urban and industrial cities (Site I); Primorskaya, which is located on the Asian continent side apart from large pollution sources (Site II); and Oki, Sado-seki and Tappi, which are located east of the Sea of Japan and are far from large pollution sources (Site III). As can be seen in Fig. 1*D*, the highest HNO_3 concentrations were observed at Site I and the highest HCl concentrations at Site III. Both HNO_3 and HCl concentrations at Site II were relatively low.

The main source of gaseous HNO_3 is the oxidation of NO_x, which is largely attributed to anthropogenic emissions from combustion of fossil fuels and production and use of fertilizers (29); hence, the highest HNO_3 concentrations at Site I would be attributable to anthropogenic emissions from the urban and industrialized area of the Asian continent.

On the other hand, the main source of gaseous HCl is volatilization from sea salt particles (e.g., heterogeneous reactions of sea salt with HNO_3 and H_2SO_4), followed by combustion of fossil fuels and occasional volcanic eruptions (30). Therefore, the highest HCl concentrations at

6

Site III would probably be induced by emissions of HCl from chemically-aged (i.e., acidified) sea salt particles suspending in the marine boundary layer over the Sea of Japan. In Fig. 3, we show an example of sea salt particles collected in an Asian dust storm that contained Ca- and Cl-rich dust particles (this sample was collected at Kanazawa on May 21, 2010). As shown here, most of the sea salt particles became depleted of Cl, suggesting the release of HCl into the atmosphere. Unfortunately, the EDX analysis used here cannot determine whether Cl-depleted sea salt particles contained N or not (see Materials and Methods). However, given that these sea salt particles contained less S, we speculate that the Cl depletion would be caused by the uptake of HNO_3 rather than that of H_2SO_4 (see also ref. 26).

Comparison with Gaseous HNO_3 and HCl at Equilibrium. It is generally thought that $Ca(NO_3)_2$ and $CaCl_2$ are formed from the heterogeneous reactions of $CaCO_3$-containing particles with HNO_3 and HCl as follows (17):

$$CaCO_{3(s)} + 2HX_{(g)} \rightarrow CaX_{2(aq)} + H_2O_{(aq)} + CO_{2(g)} \qquad [1]$$

where X is NO_3 or Cl. In addition, it should be noted here that nitrate and chloride are capable of coexisting in the same Ca-rich dust particles (31, 32). Here, we hypothesized that $Ca(NO_3)_2$ and $CaCl_2$ could form an equilibrium mixture. The equilibrium reaction between $Ca(NO_3)_2$ and $CaCl_2$ would be expressed as follows:

$$Ca(NO_3)_{2(aq)} + 2HCl_{(g)} \leftrightarrow CaCl_{2(aq)} + 2HNO_{3(g)} \qquad [2]$$
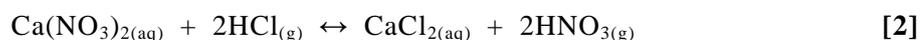
Since the Gibbs free energy change for reaction **2** is very small (1.238 kJ mol^{-1}), this reaction is, in principle, reversible.

The concentrations of gaseous HNO_3 and HCl at equilibrium for reaction **1** ($[HNO_3]_e$ and $[HCl]_e$, respectively) have been determined based on a thermodynamic calculation (see *SI Text*). In Fig. S1 *A* and *B*, we show the $[HNO_3]_e$ and $[HCl]_e$ curves under given conditions of the

7

atmospheric boundary layer (0-30°C and 40-100%RH at 1000 mbar). Both of the $[HNO_3]_e$ and $[HCl]_e$ decrease exponentially with decreasing temperature and with increasing RH. In addition, the ratios of HNO_3 to HCl at equilibrium for reaction **2**, $[HNO_3/HCl]_e$, have also been calculated (see *SI Text*) and the results are presented in Fig. S1*C*. On the basis of the $[HNO_3]_e$, $[HCl]_e$ and $[HNO_3/HCl]_e$, we examined whether the formation of $Ca(NO_3)_2$ and $CaCl_2$ through reactions **1** and **2** are thermodynamically favorable under given conditions. The relationship of $[HNO_3]_e$, $[HCl]_e$ and $[HNO_3/HCl]_e$ at 20°C is summarized in Fig. 4*A* (those at 0, 10 and 30°C are also presented in Figs. S2, S3 and S4, respectively).

The concentrations of HNO_3 and HCl measured at Sites I and III are presented in Fig. 4*B* (see also Figs. S2-S4). At all monitoring sites, the HNO_3 and HCl concentrations tended to be greater than the relevant $[HNO_3]_e$ and $[HCl]_e$, respectively. The present results suggest that reaction **1** can proceed in the forward direction for most conditions of the atmospheric boundary layer in East Asia, and a driving force exists for the production of $Ca(NO_3)_2$ and/or $CaCl_2$ from $CaCO_3$. It is important to note that the direction of reaction **2** can be determined by the proportion of HNO_3 to HCl. The highest HNO_3/HCl ratios of >1.0 were detected at Site I. The values were much greater than the relevant $[HNO_3/HCl]_e$, regardless of ambient temperature and RH. In this regime, the production of $CaCl_2$ should be always suppressed, and thus the formation of $Ca(NO_3)_2$ would be the dominant process. In contrast, the HNO_3/HCl ratios were very low at Site III and there was no significant difference among Oki, Sado-seki and Tappi. For the HNO_3/HCl ratios of ~0.1 to 0.3 at Site III, the formation of an equilibrium mixture of $Ca(NO_3)_2$ and $CaCl_2$ is preferable. In this regime, the preferred direction of reaction **2** depends mainly on ambient RH.

Discussion

The application of the equilibrium thermodynamic predictions promises to provide new insight into the conversion of Ca-rich dust particles into aqueous droplets in the atmospheric boundary layer. We suggest that the high HCl concentrations and the lowering of the HNO_3/HCl ratios at Site III (Fig. 1*D*) would allow $CaCl_2$ to be formed through reactions **1** and/or **2**. The formation of chloride in Ca-rich dust particles as measured at Kanazawa (Figs. 1*C*, 2 and 3) would be induced

8

by the reactions with HCl in the process being transported in the marine boundary layer over the Sea of Japan. We have shown that these dust particles contained almost no sulfates (see Figs. 2 and 3, and ref. 26). In addition, considering relatively moist conditions in the marine boundary layer (usually, >60%RH), it is highly likely that the production of $CaCl_2$ exceeds that of $Ca(NO_3)_2$ under most conditions around Site III. This tendency is also expected from previous *in situ* measurements of an Asian dust storm event on a ship in the Sea of Japan using an aerosol time-of-flight mass spectrometry (ATOFMS) (31, 32). Furthermore, the SEM/EDX images of Ca-rich dust particles as shown in Figs. 1*C*, 2 and 3 provide strong evidence for the involvement of aqueous $CaCl_2$ solutions in the formation process of a deliquescent layer on the particle surfaces.

On the other hand, a number of previous studies have focused mostly on the conversion of solid $CaCO_3$ into aqueous $Ca(NO_3)_2$ solutions through reaction **1** (14, 15, 19-25, 33-37), and field evidence for the existence of Ca-rich dust particles coated with highly soluble nitrate have supported the importance of this reaction in the vicinity of the urban and industrialized areas of the Asian continent (22-25). It is expected that the HNO_3 and HCl concentrations in the atmospheric boundary layer of Chuncheon are similar to those of Site I (Fig. 1*D*). Unfortunately, the HNO_3 and HCl concentrations in the urban boundary layer of eastern China (e.g., Beijing) remain to be reported, but the HNO_3/HCl ratios are presumably equal to or more than those of Site I. Hence, the absence of chloride in Ca-rich dust particles that have a droplet-like shape as measured at Beijing and Chuncheon (see Fig. 1*B* and ref. 24) would be caused by the enhanced formation of $Ca(NO_3)_2$ in dust particles under high HNO_3/HCl conditions, thus suppressing the formation of $CaCl_2$ in the same particles.

Although nitrate and chloride can coexist preferentially in the same Ca-rich dust particles under certain atmospheric conditions, the modification of the particles by stronger acids may prevent the formation of nitrate and/or chloride (26, 31, 32). An example is the reaction of them with SO_2 to form sulfate-containing dust particles (e.g., gypsum), which are less hygroscopic and remain their crystalline morphology below ~100%RH (38). However, this reaction can proceed efficiently only under extremely humid conditions (>90%RH), which are relatively rare

conditions except in the case of cloud processing (37). Therefore, we believe that the uptake of HNO_3 and HCl by dust particles is much more efficient than that of SO_2 under typical conditions of the atmospheric boundary layer, as suggested by Ooki and Uematsu (39).

The present results highlight an important mechanism for the formation of soluble materials on dust particles through heterogeneous pathways, which are possible under less polluted marine atmospheric conditions. Similar to other acids, HCl emitted from sea salt particles should be useful for acidifying the surfaces of dust particles and also for enhancing their hygroscopicity (18) and metal dissolution properties (40). However, despite the recent rapid development of chemical transport modeling studies on the reactions of dust particles with acidic gases induced by human activity (particularly HNO_3 and SO_2), the influence of high HCl concentrations in the remote marine boundary layer has not yet been considered in the model calculations (28 and references therein). Further studies will be needed to evaluate the efficiency of reactions **1** and **2**, and their relationship with other competing reactions under various conditions. Nevertheless, the current study is an important step toward establishing an understanding of the formation of aqueous solution droplets in dust storms without severe air pollution effects, as well as studying their impacts on both unidentified aerosol-cloud-climate feedback systems and ecosystems.

Materials and Methods

The size, morphology and elemental composition of individual particles found in the samples collected at Beijing ($22, 23$) and Kanazawa (26) during Asian dust storm periods were examined manually using SEM/EDX analysis. The relative composition of elements (atomic percent) with atomic number (Z) ≥ 11 in each particle was calculated using ZAF matrix correction (for this reason, the relative composition of low-Z elements such as C, N and O was not determined). On the basis of the patterns in the relative compositions, the analyzed particles were classified into several types and then only sea salt-free dust particles meeting the criterion of "Al + Si + Fe > 0", "Na ≈ 0" and "Mg < Si" (26) were examined. In this study, we applied this criterion not only to the samples collected at Beijing and Kanazawa, but also to those at Chuncheon reported by Hwang and Ro (25).

Monitoring of HNO_3 and HCl was conducted by the Acid Deposition Monitoring Network in East Asia (EANET) using a four-stage filter pack method (see Technical document for filter pack method in East Asia available at www.eanet.cc/product/techdoc_fp.pdf). The values at each monitoring site were obtained from weekly or biweekly sampling, whereas those at Kanghwa and Imsil were from daily sampling. After removing aerosol particles on the first stage (a polytetrafluoroethylene filter), all HNO_3 and partial HCl were collected on the second stage (a polyamide filter) and the remaining HCl was obtained from the third stage (a cellulose filter impregnated by K_2CO_3). Typical flow rate for weekly or biweekly sampling is ~1.0 L min^{-1}, and that for daily sampling is ~15 L min^{-1}. The concentrations of these gases were measured in aqueous filter extracts by ion chromatography. More detailed information concerning the EANET data is available via the Internet at www.eanet.cc/product.html. The procedures for calculating $[HNO_3]_e$, $[HCl]_e$ and $[HNO_3/HCl]_e$ are provided in *SI Text*.

Acknowledgements

References

1. Prospero JM (1999) Long-range transport of mineral dust in the global atmosphere: Impact of African dust on the environment of the southeastern United States. *Proc Natl Acad Sci USA* 96:3396-3403.

2. Uno I, et al. (2009) Asian dust transported one full circuit around the globe. *Nat Geosci* 2:557-560.

3. Satheesh SK, Moorthy KK (2005) Radiative effects of natural aerosols: A review. *Atmos Environ* 39:2089-2110.

4. Andreae MO, Rosenfeld D (2008) Aerosol-cloud-precipitation interactions. Part 1. The nature and sources of cloud-active aerosols. *Earth-Sci Rev* 89:13-41.

5. Baker AR, Kelly SD, Biswas FK, Witt M, Jickells TD (2003) Atmospheric deposition of nutrients to the Atlantic Ocean. *Geophys Res Lett* 30:2296 doi:10.1029/2003GL018518.

6. Paytan A, et al. (2009) Toxicity of atmospheric aerosols on marine phytoplankton. *Proc Natl Acad Sci USA* 106:4601-4605.

7. DeMott PJ, et al. (2003) Measurements of the concentration and composition of nuclei for cirrus formation. *Proc Natl Acad Sci USA* 100:14655-14660.

8. Pratt KA, et al. (2009) *In situ* detection of biological particles in cloud ice-crystals. *Nat Geosci* 2:398-401.

9. Möhler O, et al. (2008) The effect of organic coating on the heterogeneous ice nucleation efficiency of mineral dust aerosols. *Environ Res Lett* 3:025007 doi:10.1088/1748-9326/3/2/025007.

10. Eastwood ML, et al. (2009) Effects of sulfuric acid and ammonium sulfate coatings on the ice nucleation properties of kaolinite particles. *Geophys Res Lett* 36:L02811 doi:10.1029/2008GL035997.

11. Levin Z, Ganor E, Gladstein V (1996) The effects of desert particles coated with sulfate on rain formation in the eastern Mediterranean. *J Appl Meteorol* 35:1511-1523.

12. Levin Z, Teller A, Ganor E, Yin Y (2005) On the interactions of mineral dust, sea-salt particles, and clouds: A measurement and modeling study from the Mediterranean Israeli

Dust Experiment campaign. *J Geophys Res* 110:D20202 doi:10.1029/2005JD005810.

13. Kelly JT, Chuang CC, Wexler AS (2007) Influence of dust composition on cloud droplet formation. *Atmos Environ* 41:2904-2916.

14. Gibson ER, Hudson PK, Grassian VH (2006) Aerosol chemistry and climate: Laboratory studies of the carbonate component of mineral dust and its reaction products. *Geophys Res Lett* 33:L13811 doi:10.1029/2006GL026386.

15. Gibson ER, Hudson PK, Grassian VH (2006) Physicochemical properties of nitrate aerosols: Implications for the atmosphere. *J Phys Chem A* 110:11785-11799.

16. Lack DA, et al. (2009) Relative humidity dependence of light absorption by mineral dust after long-range atmospheric transport from the Sahara. *Geophys Res Lett* 36:L24805 doi:10.1029/2009GL041002.

17. Kelly JT, Wexler AS (2005) Thermodynamics of carbonates and hydrates related to heterogeneous reactions involving mineral aerosol. *J Geophys Res* 110:D11201 doi:10.1029/2004JD005583.

18. Sullivan RC, et al. (2009) Effect of chemical mixing state on the hygroscopicity and cloud nucleation properties of calcium mineral dust particles. *Atmos Chem Phys* 9:3303-3316.

19. Krueger BJ, Grassian VH, Cowin JP, Laskin A (2004) Heterogeneous chemistry of individual mineral dust particles from different dust source regions: The importance of particle mineralogy. *Atmos Environ* 38:6253-6261.

20. Laskin A, Wietsma TW, Krueger BJ, Grassian VH (2005) Heterogeneous chemistry of individual mineral dust particles with nitric acid: A combined CCSEM/EDX, ESEM, and ICP-MS study. *J Geophys Res* 110:D10208 doi:10.1029/2004JD005206.

21. Laskin A, et al. (2005) Direct observation of completely processed calcium carbonate dust particles. *Faraday Discuss* 130:453-468.

22. Matsuki A, et al. (2005) Heterogeneous sulfate formation on dust particles and its dependence on mineralogy: Balloon-borne measurements in the surface atmosphere of Beijing, China. *Water Air Soil Pollut Focus* 5:101-132.

23. Matsuki A, et al. (2005) Morphological and chemical modification of mineral dust:

Observational insight into the heterogeneous uptake of acidic gases. *Geophys Res Lett* 32:L22806 doi:10.1029/2005GL024176.

24. Li WJ, Shao LY (2009) Observation of nitrate coatings on atmospheric mineral dust particles. *Atmos Chem Phys* 9:1863-1871.

25. Hwang HJ, Ro C-U (2006) Direct observation of nitrate and sulfate formations from mineral dust and sea-salts using low-*Z* particle electron probe X-ray microanalysis. *Atmos Environ* 40:3869-3880.

26. Tobo Y, et al. (2009) Hygroscopic mineral dust particles as influenced by chlorine chemistry in the marine atmosphere. *Geophys Res Lett* 36:L05817 doi:10.1029/2008GL036883.

27. Sun J, Zhang M, Liu T (2001) Spatial and temporal characteristics of dust storms in China and its surrounding regions, 1960-1999: Relations to source area and climate. *J Geophys Res* 106:10325-10333.

28. Fairlie TD, et al. (2010) Impact of mineral dust on nitrate, sulfate, and ozone in transpacific Asian pollution plumes. *Atmos Chem Phys* 10:3999-4012.

29. Duce RA, et al. (2008) Impacts of atmospheric anthropogenic nitrogen on the open ocean. *Science* 320:893-897.

30. Graedel TE, Keene WC (1995) Tropospheric budget of reactive chlorine. *Global Biogeochem Cycles* 9:47-77.

31. Sullivan RC, Guazzotti SA, Sodeman DA, Prather KA (2007) Direct observations of the atmospheric processing of Asian mineral dust. *Atmos Chem Phys* 7:1213-1236.

32. Sullivan RC, et al. (2007) Mineral dust is a sink for chlorine in the marine boundary layer. *Atmos Environ* 41:7166-7179.

33. Usher CR, Michel AE, Grassian VH (2003) Reactions on mineral dust. *Chem Rev* 103:4883-4939.

34. Vlasenko A, et al. (2006) Effect of humidity on nitric acid uptake to mineral dust aerosol particles. *Atmos Chem Phys* 6:2147-2160.

35. Liu Y, et al. (2008) Kinetics of heterogeneous reaction of $CaCO_3$ particles with gaseous

HNO$_3$ over a wide range of humidity. *J Phys Chem A* 112:1561-1571.

36. Sullivan RC, et al. (2009) Timescale for hygroscopic conversion of calcite mineral particles through heterogeneous reaction with nitric acid. *Phys Chem Chem Phys* 11:7826-7837.

37. Preszler Prince A, et al. (2007) Heterogeneous interactions of calcite aerosol with sulfur dioxide and sulfur dioxide-nitric acid mixtures. *Phys Chem Chem Phys* 9:3432-3439.

38. Shi Z, et al. (2008) Influences of sulfate and nitrate on the hygroscopic behavior of coarse dust particles. *Atmos Environ* 42:822-827.

39. Ooki A, Uematsu M (2005) Chemical interactions between mineral dust particles and acidic gases during Asian dust events. *J Geophys Res* 110:D03201 doi:10.1029/2004JD004737.

40. Rubasinghege G, Lentz RW, Scherer MM, Grassian VH (2010) Simulated atmospheric processing of iron oxyhydroxide minerals at low pH: Roles of particle size and acid anion in iron dissolution. *Proc Natl Acad Sci USA* 107:6628-6633.

Figure Legends

Fig. 1. Information on field measurements of chemically-aged dust particles and reactive acidic gases in East Asia. (*A*) Location of the measurement sites. Red contour lines show the regions where calcium nitrate formation involving dust particles tends to be strongly activated (28). (*B*) Relative atomic ratios of Ca:Cl:(Al + Si + Fe) for dust particles collected at Beijing (22), and SEM images of typical Ca-free and Ca-rich particles taken using 10 kV electron beam (Scale bar, 3 μm). The relative atomic ratios for dust particles collected at Chuncheon (25) are also shown for reference. (*C*) Same as Fig. 1*B*, but for the particles collected at Kanazawa (26). (*D*) Ground-based measurements of gaseous HNO_3 and HCl at Kanghwa (*n* = 13), Imsil (*n* = 12), Primorskaya (*n* = 6), Oki (*n* = 7), Sado-seki (*n* = 7) and Tappi (*n* = 7) from March to May 2007 (means ± standard deviations).

Fig. 2. SEM/EDX images of dust particles that contain rich Ca, Cl, Si and Al collected at Kanazawa during an Asian dust storm event. (*A*) SEM images of the particles taken using 5 and 20 kV electron beams. (*B*) EDX spectra from selected parts (I and II) in Fig. 2*A*. Ni in spectra is from the mesh grid. (*C*) Structure of a representative of the particles inferred from SEM/EDX analysis.

Fig. 3. SEM/EDX images of dust and sea salt particles collected at Kanazawa during an Asian dust storm event. (*A*) SEM images of the particles taken using 5 and 20 kV electron beams. (*B*) Three element (Ca, Cl and Na) mapping of these particles. (*C*) EDX spectra from these individual particles. Ni in spectra is from the mesh grid.

Fig. 4. Relationship of the concentration of HNO_3 and HCl with reactions **1** and **2**. (*A*) RH dependence of $[HNO_3]_e$, $[HCl]_e$ and $[HNO_3/HCl]_e$ at 20°C. (*B*) Measured values of HNO_3 and HCl at Kanghwa, Imsil, Oki, Sado-seki and Tappi from March to May 2007. Note: if ambient HNO_3 concentrations are greater than $[HNO_3]_e$ and the ratios of HNO_3 to HCl are greater than $[HNO_3/HCl]_e$, then the reactions to form $Ca(NO_3)_2$ are thermodynamically favorable.